

Four-wave mixing in silicon coupled-cavity resonators with port-selective, orthogonal supermode excitation

Xiaoge Zeng,^{1,*} Cale M. Gentry,² and Miloš A. Popović²

¹*Department of Physics, University of Colorado, Boulder, Colorado 80309, USA*

²*Department of Electrical, Computer, and Energy Engineering, University of Colorado, Boulder, Colorado 80309, USA*

*Corresponding author: xiaoge.zeng@colorado.edu

Received December 29, 2014; revised April 7, 2015; accepted April 7, 2015;
posted April 8, 2015 (Doc. ID 234778); published May 1, 2015

We propose coupled-cavity triply-resonant systems for degenerate-pump four-wave mixing (FWM) applications that support strong nonlinear interaction between distributed pump, signal and idler modes, and allow independent coupling of the pump mode and signal/idler modes to separate ports based on nonuniform supermode profile. We demonstrate seeded FWM with wavelength conversion efficiency of -54 dB at input pump power of 3.5 dBm, and discuss applications of such orthogonal supermode coupling. © 2015 Optical Society of America
OCIS codes: (190.4380) Nonlinear optics, four-wave mixing; (130.4310) Nonlinear.
<http://dx.doi.org/10.1364/OL.40.002120>

Nonlinear optical interaction can be resonantly enhanced in microcavities with small mode volumes and high-field enhancements. Degenerate-pump four-wave mixing (FWM), for example, favors triply resonant cavities [1]. A single microring cavity used for FWM, with three interacting waves at different longitudinal order resonances, has a trade-off between mitigating dispersion by using a large ring and enhancing nonlinear interaction with small mode volume [2]. The design also constrains the choice of pump, signal, and idler wavelengths.

Since the minimum number of modes required for FWM is three, one can avoid the constraints imposed by using multiple longitudinal modes of a single cavity by instead coupling three cavities together where the interacting signal, pump, and idler wavelengths each excite a compound resonance of the coupled-cavity resonator. Both stimulated and spontaneous FWMs have been demonstrated in a triple-cavity resonator [3,4]. In these devices, however, the external ports (bus waveguides) couple to all resonance modes with fixed ratio of coupling rates, leading to undesirable crosstalk or reduced efficiency. The use of more than three coupled resonators has also been investigated in coupled-resonator optical waveguides (CROW) [5–7] taking advantage of reduced group velocity and broad passband.

A desirable quality of a resonant four-wave mixing device is separate and independent waveguide coupling to the three interacting modes in order to both engineer the linewidths/decay rates (and therefore field enhancement) of each resonant mode along with intrinsic isolation between the input pump and generated signal/idler light. Optimum design of an optical parametric oscillator calls for unequal coupling of the waveguide(s) to the three resonances that interact via FWM [8,9]. Also, in parametric wavelength conversion and/or amplification of an optical data stream, to maximally utilize a CW pump, we suggest that a narrow-linewidth pump resonance should be used to minimize the needed pump power, while high bit-rate data streams require wide-linewidth signal and idler resonances to accommodate the modulated signals. It is also advantageous in a photon

pair generator to critically couple the pump mode while the signal/idler modes are over-coupled to promote both efficiency and photon time correlation. While controllable mode-selective coupling was recently proposed [8] and partially demonstrated [4], the latter work still couples two modes to one port and all three to another port resulting in the generated correlated photons being randomly and uncontrollably routed to two different output ports.

In this report, we demonstrate orthogonal coupling of supermodes in a triple-cavity resonator to two separate bus waveguides, show stimulated FWM in such a device, and propose broad applications based on it. In general, independent orthogonal excitation of all three resonances would require three separate bus waveguides, with each coupled exclusively to one of the three resonances. Here we present a more restricted design where the pump is independently controlled from the signal and idler. This design is suitable to degenerate FWM because signal and idler physics are symmetric. The device enables breaking the trade-off between increasing parametric gain (by reducing volume) and mitigating dispersion, as well as the choice of wavelengths by design, with independently designable coupling to the resonances. We demonstrate four-wave mixing for the first time in such a device, and discuss potential applications.

The “photonic molecule” compound resonator consists of three identical microcavities in series (which could be microdisks/rings, photonic crystal cavities, or microcavities of other geometry), and two bus waveguides [see Fig. 1(a)]. Direct coupling of three identical cavities with two equal coupling strengths μ forms three supermodes resonant at $\omega_o - \mu\sqrt{2}$, ω_o , and $\omega_o + \mu\sqrt{2}$, where ω_o is the angular resonant frequency of a single microcavity. The frequency spacing of the supermodes is controlled by the cavity-cavity coupling set by the geometric gap between adjacent cavities. The field of each supermode is distributed across the cavities [Fig. 1(b)] with field amplitudes in each cavity akin to a discrete version of the (1-, 2- and 3-half-wavelength) wavefunctions of a particle-in-a-box-potential in the three lowest

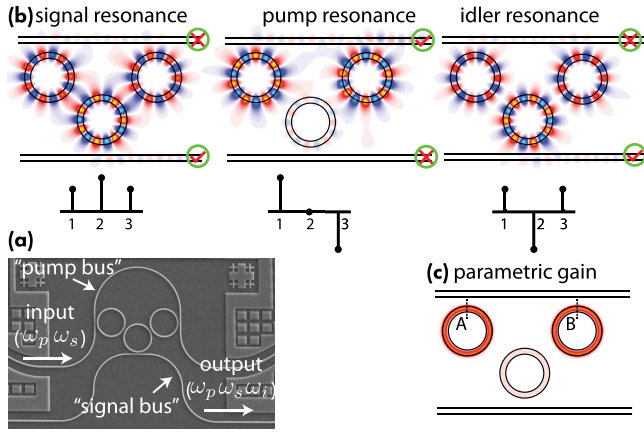


Fig. 1. Proposed “photonic molecule” resonator with port-selective, orthogonal supermode coupling: (a) SEM of triple-ring resonator with a “signal bus” coupled to the middle cavity and a “pump bus” interferometrically coupled to the outer cavities; (b) simulated field of signal, pump, and idler resonances including decay to ports, showing suppressed coupling of signal bus to pump resonance and pump bus to signal/idler resonances. (c) simulated parametric gain distribution of degenerate FWM.

energy eigenstates. Therefore when used to enhance signal ($\omega_s = \omega_o - \mu\sqrt{2}$), pump ($\omega_p = \omega_o$), and idler ($\omega_i = \omega_o + \mu\sqrt{2}$) wavelengths in a degenerate FWM process, these three supermodes automatically satisfy both photon energy conservation ($2\omega_p = \omega_s + \omega_i$) and phase matching ($2k_p = k_s + k_i$) conditions. Unlike a single-ring resonator, a triple-ring resonator does not require careful design of waveguide cross-section dimension to minimize dispersion for phase matching—the three supermodes of the same longitudinal order in triple cavities automatically satisfy it as long as the rings are identical and couplings are small. However, since the three modes have different mode profiles, their effective overlap volume for FWM is four times as large as that of a single microring [9]. This efficiency reduction may serve as a necessary trade off for the additional flexibility in design. A plot of parametric gain distribution in the triple-ring cavity is shown in Fig. 1(c). There is little parametric gain in the middle cavity. It should be noted that the triple-ring cavity system for FWM is different from third-order bandpass filters composed of three rings. The former has well-resolved resonances with a frequency spacing larger than the linewidth of each supermode, while the latter typically have supermode linewidths that are larger than their frequency spacing [10].

We next engineer the couplings of two waveguides to the compound resonator to be mode-selective. As Fig. 1(b) shows, the pump resonance has nearly zero energy in the middle cavity, and thus barely couples to the bottom bus, which is only coupled to the middle cavity. However, the signal and idler resonances have significant field in the middle cavity and couple to the bottom bus (which we shall call the “signal bus”). Next, the top bus (we shall call it the “pump bus”) couples equally to the two outer cavities via two coupling points [see point A and B in Fig. 1(c)]. The phase difference of the pump mode field at these two coupling points are shifted by π relative to that of the signal/idler mode ($\Delta\phi_{AB}^p - \Delta\phi_{AB}^{s/i} = \pi$). Then the length of the section of “pump

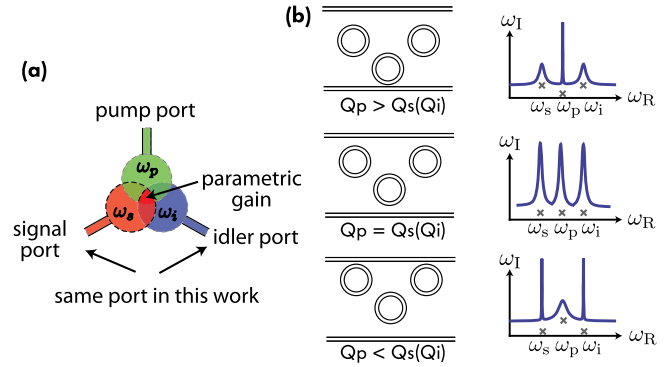


Fig. 2. (a) Cartoon illustrating mode-selective coupling to ports; (b) effect of choices of the “pump bus” and “signal bus” gaps in the proposed orthogonal supermode linewidth engineering scheme.

bus” between these two coupling points can be designed so that the “pump bus” couples destructively to the signal and idler resonances, while coupling optimally to the pump resonance. As a result, the external couplings to the pump and signal/idler resonances are entirely isolated to separate waveguides, with a “pump bus” waveguide solely for pump resonance excitation and a “signal bus” waveguide solely for signal/idler resonance coupling. The device in the linear regime is an all-pass filter on each bus—the only source of power transfer from the pump bus to the signal/idler bus is the nonlinear (FWM) coupling. This allows control of geometric gaps to independently control the pump and signal/idler linewidths (see Fig. 2), while intrinsically filtering the pump from the signal/idler bus in principle.

To demonstrate the concept, triple-ring resonators were fabricated on SOI wafers with a 220-nm device layer through the ePIXfab foundry service [11]. A ring radius of $3.5 \mu\text{m}$ was chosen to minimize mode volume without compromising the quality factor (Q) through bending loss. Due to lithographic and device layer thickness variations, the three rings can have different resonance frequencies, resulting in unequal frequency spacing between the supermodes ($2\omega_p \neq \omega_s + \omega_i$). In addition, coupling-induced frequency shifts can also cause unequal frequency spacing when the coupling gaps are small since light in the middle ring sees a different environment than that in the outer rings [12]. To compensate for any frequency mismatch, resistive metal microheaters were fabricated on top of the oxide top cladding to thermally tune the compound resonator elements. Each ring was tuned independently to restore the designed supermode, and the interferometric phase in the “pump bus” was tuned to control its coupling to each supermode. Fabricated triple-ring cavities with microheaters are shown in Fig. 3(a). The heaters were fabricated in a two-step procedure involving scanning electron-beam lithography to enable fine features, and contact photolithography for the larger pads.

Figure 3(b) shows passive spectra of a triple-ring resonator, where the insertion loss is plotted against swept laser wavelength. The notation “ps” denotes the case when the input fiber is coupled to the “pump bus,” and the output fiber is coupled to the “signal bus,” etc.

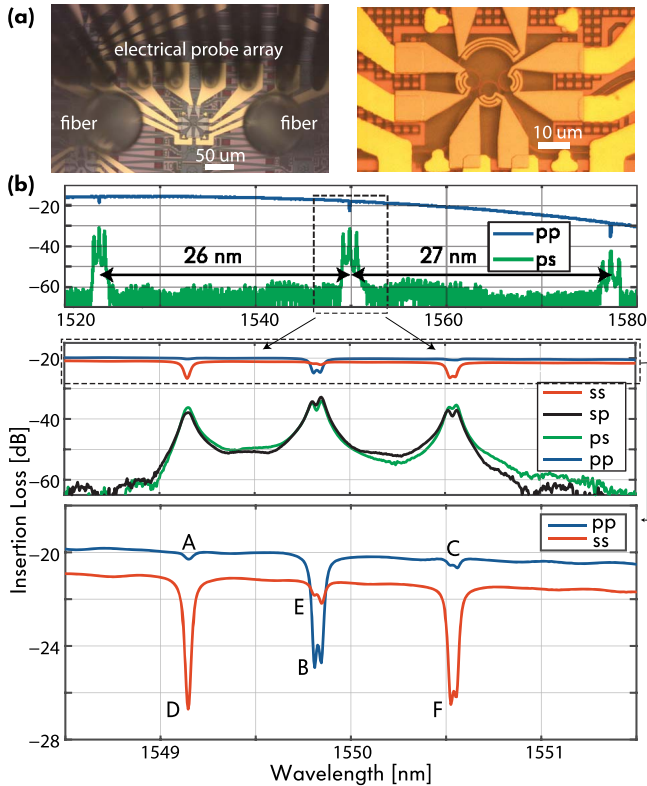


Fig. 3. (a) Micrographs of device under test with heaters; (b) optical transmission spectra of four port combinations (legend: “ps” = “pump bus” input, “signal bus” output). The little transmission dips E (A, C) show that “signal (pump) bus” couples weakly to pump (signal/idler) resonance.

The free spectral range (FSR) is nonuniform due to dispersion. However, the compound resonator has three modes with nearly equal frequency spacing within one FSR, enabling degenerate-pump FWM near 1550 nm. The spectra verified the port-selective coupling of the three supermodes. In the through port transmission of the “pump bus” (i.e., the “pp” curve), there are no substantial transmission dips at the signal/idler resonance frequency [see “A” and “C” in Fig. 3(b)], showing that coupling of the “pump bus” to the signal/idler resonance of the triple-ring cavity is frustrated, per design. Similarly the “signal bus” couples weakly to the pump resonance as indicated by the little dip at “B.” Therefore, the linewidth of the signal/idler (pump) resonance is controlled entirely via its coupling to the “signal (pump) bus” and intrinsic cavity loss, and can be engineered independently through the respective ring-bus coupling gap. The “pump bus” (“signal bus”) was designed to be critically coupled to the pump (signal/idler) resonance assuming an unloaded Q of around 150,000. However, we extracted an unloaded Q of only 50,000 from the passive spectrum [as evidenced by the small dips “D,” “F” (“B”) at signal/idler (pump) wavelength in the “signal (pump) bus” through port transmission], showing that all three resonances are under-coupled.

In the experiment, we thermally tuned the individual rings and interferometric bus to enable equally spaced supermodes, and coupled the pump and seed light resonant with the compound cavity both via the “pump” bus (the seed should enter via the signal bus, and this

nonideal excitation was governed by experimental constraints). Parametric wavelength conversion via FWM was observed at an input pump power of 3.5 dBm and seed power of -7.3 dBm in the input “pump bus.” Figure 4(a) shows the power spectrum of output light at drop port in “signal bus” measured with an optical spectrum analyzer (OSA); the apparent wide linewidths are due to the filter response of the OSA. The generated idler light power exiting in the “signal bus” at the device was estimated to be -61.3 dBm after taking into consideration the insertion loss of fiber-chip couplers. Thus the measured FWM conversion efficiency from signal light at input “pump bus” to generated idler light at the “signal bus” is approximately -54 dB at in-waveguide pump power of 3.5 dBm. Since the pump light coupling from the triple-ring cavity to the “signal bus” is frustrated by design [see Fig. 3(b), with a rejection of 13 dB], the demonstrated device works as an effective filter for the strong pump light when detecting generated signal at the “signal bus.”

To understand the limitations, efficiency scaling, and potential of this device, we study the theoretical FWM conversion efficiency taking into account the two-photon absorption (TPA) and free-carrier absorption (FCA). We assume resonant excitation of pump and seed light, as well as perfect phase matching and critical coupling for the three modes. In Fig. 4(b) we show the simulated wavelength conversion efficiency (from signal to idler light) in silicon microresonator based on degenerate-pump FWM as a function of normalized pump power

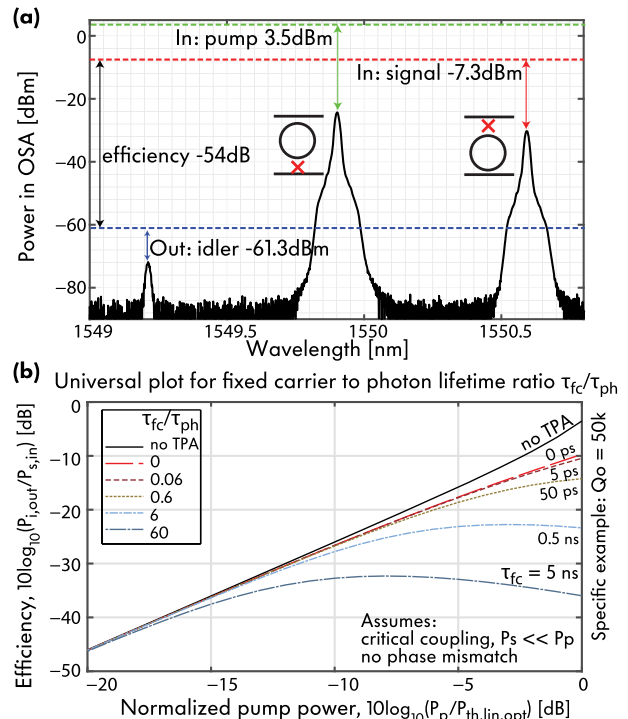


Fig. 4. (a) Seeded FWM in silicon triple-ring resonator with conversion efficiency of -54 dB. (b) Degenerate-pump FWM wavelength conversion efficiency versus normalized pump power [9] in a silicon microcavity with nonlinear loss included. Critical coupling and perfect phase matching are assumed. A few ratios of free carrier and photon lifetime are used.

[9], which is the in-bus pump power normalized to the oscillation threshold power with optimum coupling when nonlinear loss can be neglected. This oscillation threshold power scales quadratically with intrinsic cavity loss rate and linearly with nonlinear interaction mode volume. The parametric wavelength conversion efficiency decreases with the ratio of free-carrier lifetime and intrinsic cavity photon lifetime (defined as $\tau_{\text{ph}} \equiv 1/r_o$, where r_o is intrinsic cavity loss). The under-coupled configuration in our fabricated device leads to lower cavity enhancement lowering both parametric conversion and free-carrier generation via TPA. With normalized pump power of only -12.3 dB (i.e., 3.5 dBm actual power in bus) and assuming free-carrier lifetime of 1 ns, we can therefore predict that the nonlinear loss only slightly decreases the FWM efficiency in our device.

When the TPA can be neglected and conversion efficiency is small, the pump and seed are not depleted, and the FWM efficiency has a simple expression [2,9]:

$$\eta = (\omega\beta_{\text{fwm}}P_{p,\text{in}})^2 \frac{2r_{i,\text{out}}}{\Delta\omega_i^2 + r_{i,t}^2} \frac{2r_{s,\text{in}}}{\Delta\omega_s^2 + r_{s,t}^2} \left(\frac{2r_{p,\text{in}}}{\Delta\omega_p^2 + r_{p,t}^2} \right)^2,$$

where β_{fwm} is the FWM coefficient in the resonator, which is inversely proportional to the nonlinear interaction mode volumes, $P_{p,\text{in}}$ is the input pump power in the “pump bus,” $r_{k,t}$ ($k \in \{s, p, i\}$) is total loss rate for resonance ω_k , and $\Delta\omega_k$ is the frequency detuning of the excitation from the corresponding resonance. $r_{p,\text{in}}$ and $r_{s,\text{in}}$ are coupling rates from the “pump bus” to the resonator at the pump and signal frequencies, and $r_{i,\text{out}}$ is the coupling rate from the resonator to the “signal bus” at the idler frequency. Maximum efficiency is achieved with critical coupling at the input bus for the pump and seed light, and at the output bus for the idler light. However, as Fig. 3(b) shows, our device is under-coupled, with measured unloaded Q of $50,000$ and external Q of $120,000$ – $170,000$. Furthermore, the signal light was inserted via the “pump bus” due to experimental constraints (using the same input fiber as the pump), *not* in the “signal bus” as is optimal. Therefore, the signal light is very poorly coupled into the resonator. With the actual weak external couplings, the theory predicts a conversion efficiency of -47.3 dB, which is 6.7 dB higher than the measured -54 dB. The remaining difference, we believe, is due to excitation of nonideal supermodes, resonance splitting due to the coupling of two counter-propagating traveling-wave in the rings, FCA, phase mismatch, and inaccuracy in estimating external couplings.

When the nonlinear loss can be neglected, the stimulated FWM conversion efficiency from signal light to idler light is proportional to the square of pump power, and the ratio η/P_p^2 , pump-normalized conversion efficiency (PNCE), should be used as a figure of merit for wavelength conversion efficiency of a nonlinear mixer based on degenerate-pump FWM. This ratio was measured to be $8 \times 10^{-7} (\text{mW})^{-2}$ in our triple-ring device. Although this efficiency is smaller than those of the coupled resonator [3] and microring resonator with active carrier removal [13], we have demonstrated here the feasibility of performing FWM in a triple-ring resonator with separate bus waveguides coupling to the pump

and signal/idler modes, enabling different linewidths for these modes. By launching the pump and seed light into separate input ports as intended, and ensuring critical coupling, we expect the efficiency in this device to increase by 20 dB to around -34 dB. This can be accomplished by providing separate grating couplers into the pump bus and signal bus input ports, in a geometry accessible by two separate input fibers carrying the pump and seed signal. Alternatively, a 2D grating coupler could take the pump and signal from orthogonal polarizations in the input fiber into the two bus waveguides. Last, a co-polarized pump and signal in a single fiber can be separated into the pump and signal bus by a wavelength filter on chip. By increasing the unloaded quality factor from $50,000$ to $500,000$, and sweeping out free carriers, net gain could be within reach. The unloaded Q in the present devices is limited by larger than expected sidewall roughness on the ring cavities, and coupler radiation loss. These factors are being currently addressed in revised designs and pose no fundamental limitation.

In summary, we have proposed and demonstrated coupled-cavity structures for resonantly enhanced four-wave mixing that enable independent coupling of pump, signal, and idler resonances to separate ports. We expect it to enable an array of applications including optimum designs for parametric amplifiers, oscillators, squeezing, and photon pair generation including engineering of the biphoton joint spectral distribution.

This work was supported by a 2012 Packard Fellowship for Science and Engineering (Grant No. 2012-38222), and by Office of Naval Research Grant N000141410259.

References

1. D. M. Ramirez, A. W. Rodriguez, H. Hashemi, J. D. Joannopoulos, M. Soljačić, and S. G. Johnson, *Phys. Rev. A* **83**, 033834 (2011).
2. C. M. Gentry, X. Zeng, and M. A. Popović, *Opt. Lett.* **39**, 5689 (2014).
3. A. H. Atabaki and A. Adibi, “Demonstration of wavelength conversion in a reconfigurable coupled resonator in silicon,” in *Photonics Conference (PHO)* (IEEE, 2011), pp. 399–400.
4. S. Azzini, D. Grassani, M. Galli, D. Gerace, M. Patrini, M. Liscidini, P. Velha, and D. Bajoni, *Appl. Phys. Lett.* **103**, 031117 (2013).
5. F. Morichetti, A. Canciamilla, C. Ferrari, A. Samarelli, M. Sorel, and A. Melloni, *Nat. Commun.* **2**, 296 (2011).
6. J. R. Ong, M. L. Cooper, G. Gupta, W. M. Green, S. Assefa, F. Xia, and S. Mookherjea, *Opt. Lett.* **36**, 2964 (2011).
7. R. Kumar, J. R. Ong, J. Recchio, K. Srinivasan, and S. Mookherjea, *Opt. Lett.* **38**, 2969 (2013).
8. X. Zeng and M. A. Popović, “Optimum micro-optical parametric oscillators based on third-order nonlinearity,” in *CLEO: Science and Innovations* (Optical Society of America, 2013), paper CTh1F7.
9. X. Zeng and M. A. Popović, *Opt. Express* **22**, 15837 (2014).
10. B. E. Little, S. T. Chu, H. A. Haus, J. Foresi, and J.-P. Laine, *J. Lightwave Technol.* **15**, 998 (1997).
11. ePIXfab Multi-Project Wafer Service for Silicon Photonics, www.epixfab.eu.
12. M. Popović, C. Manolatou, and M. Watts, *Opt. Express* **14**, 1208 (2006).
13. J. R. Ong, R. Kumar, R. Aguinaldo, and S. Mookherjea, *IEEE Photon. Technol. Lett.* **25**, 1699 (2013).